

The crystal structure and chemical composition of cumengéite

F. C. HAWTHORNE AND L. A. GROAT

Department of Earth Sciences, University of Manitoba, Winnipeg, Manitoba, Canada, R3T 2N2

ABSTRACT. The crystal structure of cumengéite, $\text{Pb}_{21}\text{Cu}_{20}\text{Cl}_{42}(\text{OH})_{40}$, tetragonal, $a = 15.065(2)$, $c = 24.436(5)$ Å, $V = 5546(2)$ Å³, space group $I4/mmm$, $Z = 2$, has been solved by direct methods and refined by least-squares to an R index of 7.1% for 1158 observed ($I > 2.5\sigma(I)$) reflections. The cumengéite structure shows a very diverse range of cation coordinations. There are five distinct Pb sites with the following coordination polyhedra: octahedron, square antiprism, augmented trigonal prism, a very distorted biaugmented trigonal prism and a fairly regular biaugmented trigonal prism, the latter being only half-occupied; there are two distinct Cu sites with octahedral and square pyramidal coordination respectively. The coordination polyhedra share elements to form prominent columns or rods of polyhedra parallel to the c -axis and centred on the 4-fold axes of the unit cell. These rods form a body-centred array, and link by sharing elements of their coordination polyhedra.

KEYWORDS: cumengéite, crystal structure.

CUMENGÉITE is a lead copper hydroxy-chloride mineral occurring in the oxidized zones of hydrothermal lead copper sulphide deposits. It is typically associated with other minerals of the boléite group, the mineralogy of which has been reviewed by Winchell and Rouse (1974). Dean *et al.* (1983) report a new occurrence from Cornwall, and Humphreys *et al.* (1980) and Abdul-Samad *et al.* (1981) have investigated the stability of the boléite group minerals. Rouse (1973) solved the crystal structure of boléite, but the details of the other structures are not known. The recent resurgence of interest in the boléite minerals prompted this study on the structure of cumengéite.

Experimental

The material used in this study is from Boleo, Baja California, Mexico, and has now been deposited at the Department of Mineralogy and Geology, Royal Ontario Museum, Toronto, catalogue number M41630. The sample, a single crystal ~ 2 mm in the longest dimension, was crushed and several fragments were mounted in epoxy and

polished for electron microprobe analysis. The analysis was done on a MAC 5 instrument operating in the energy dispersive mode using a Kevex Micro-X 7000 analytical spectrometer with a Si(Li) detector and a 1024 channel multichannel analyser operated at 10 eV per channel. The specimen current, measured on fayalite, was 10 na at 15 kV, and the collection time was 200 live seconds. The following standards were used: chalcopyrite (Cu), PbTe(Pb), KCl(Cl). The analysis (mean of several points) is given in Table I, and the resulting formula, normalized to 42 cations, conforms quite well to the ideal as indicated by the structure analysis.

Precession photographs displayed Laue symmetry $4/mmm$ with systematic absences $h + k + l \neq 2n$, consistent with the space groups $I4/mmm$, $I\bar{4}2m$, $I4m2$, $I4mm$ and $I422$. Long-exposure zero- and upper-level photographs confirmed the cell assigned by previous workers. The crystal initially used for the intensity data collection was an irregular equidimensional fragment ~ 0.25 mm in diameter. It was mounted on a Nicolet R3m automatic four-circle diffractometer, and twenty-five strong reflections were automatically aligned. Least-squares refinement of the setting angles produced tetragonally constrained cell dimensions very similar to the values given in Table II, together with the orientation matrix relating the crystal axes to the diffractometer axes.

Intensity data were collected according to the method of Hawthorne (1985), a total of 2732 reflections being measured over 2 asymmetric units. An empirical absorption correction was done, modelling the crystal as an ellipsoid to reduce the merging R index of the azimuthal scan data from 15.5 to 7.7%. The data were corrected for Lorentz, polarization, background and absorption effects, equivalent reflections were averaged (merging R index = 8.4%) and then reduced to structure factors; of the 1444 reflections, 1158 were classed as observed ($I > 2.5\sigma(I)$).

Scattering curves for neutral atoms together with

Table I. Electron microprobe analysis of cumengéite

Analysis		Formula unit		ideal
CuO	21.60 wt. %	Cu	20.6	20
PbO	62.84	Pb	21.4	21
Cl	18.51 102.95 -8.35	Cl	39.6	42
(H ₂ O)*	94.60 4.63 99.23			

* ideal, calculated from the structural formula.

Table III. Atomic positions for cumengéite

Atom	x	y	z	U [*] equiv.
Pb(1)	0	0	0	4.0(1)
Pb(2)	0	0	0.3199(1)	4.6(1)
Pb(3)	0.27634(9)	0	0.23459(6)	3.9(1)
Pb(4)	0.19780(6)	0.19780(6)	0.36453(6)	3.8(1)
Pb(5) [†]	1/2	0	0.4104(2)	3.9(1)
Cu(1)	0.2599(2)	0.0962(2)	0.0910(1)	3.4(1)
Cu(2)	0.2610(3)	0.2610(3)	0	3.7(1)
Cl(1)	0.1318(6)	0.1318(6)	0	5.1(4)
Cl(2)	0.3815(4)	0.1269(4)	0.1786(3)	4.5(2)
Cl(3)	0	0	0.1187(9)	4.7(5)
Cl(4)	0.1696(7)	0	0.3765(5)	6.1(4)
Cl(5)	0.1274(5)	0.1274(5)	0.2461(4)	4.9(2)
Cl(6)	0.3701(9)	0	1/2	7.2(7)
O(1)	0.3007(10)	0.1762(9)	0.4412(6)	3.2(5)
O(2)	0.1850(11)	0.1850(11)	0.1275(9)	3.8(6)
O(3)	0.2120(16)	0	0.1357(11)	3.9(7)
O(4)	0.3272(15)	0	0.0571(9)	3.7(8)

U^{*} equiv. = U_{equiv.} × 10²; † position half-occupied

Table II. Miscellaneous information: cumengéite

a	15.065(2) Å	Crystal size(mm)	0.18
c	24.436(5)	Rad/Mon	Mo/Gr
V	5546(2) Å ³	Total F _o	1444
Space Group	14/mmm	I>2.5σI	1158
D(calc)	= 4.66 gm.cm. ⁻³		
Structural formula:	2[Pb ₂₁ Cu ₂₀ Cl ₄₂ (OH) ₄₀]		
Final R(obs)	= 7.1%		
Final R _w	= 5.5%		

Table IV. Anisotropic temperature factor coefficients: cumengéite

Atom	U [*] 11	U ₂₂	U ₃₃	U ₂₃	U ₁₃	U ₁₂
Pb(1)	37(1)	37(1)	46(3)	0	0	0
Pb(2)	44(1)	44(1)	51(2)	0	0	0
Pb(3)	39(1)	37(1)	39(1)	0	0(1)	0
Pb(4)	38(1)	38(1)	38(1)	-3(1)	-3(1)	-2(1)
Pb(5)	39(2)	36(2)	40(2)	0	0	0
Cu(1)	37(2)	31(1)	35(2)	2(1)	5(1)	0(1)
Cu(2)	40(2)	40(2)	30(3)	0	0	5(3)
Cl(1)	56(5)	56(5)	40(8)	0	0	-20(7)
Cl(2)	43(4)	51(4)	42(3)	6(3)	-5(3)	-5(3)
Cl(3)	41(6)	41(6)	58(14)	0	0	0
Cl(4)	60(6)	36(5)	86(8)	0	-20(6)	0
Cl(5)	53(3)	53(3)	42(5)	7(4)	7(4)	14(4)
Cl(6)	42(8)	34(7)	139(18)	0	0	0
O(1)	37(8)	37(9)	22(7)	-4(7)	11(8)	7(7)
O(2)	44(8)	44(8)	27(12)	3(8)	3(8)	4(11)
O(3)	48(14)	25(10)	43(13)	0	-12(14)	0
O(4)	37(13)	35(12)	38(14)	0	3(12)	0

* U_{ij} = U_{ij} × 10³

anomalous dispersion coefficients were taken from Cromer and Mann (1968) and Cromer and Liberman (1970) respectively. The distribution of E-values was centric, and the space group *14/mmm* was adopted. The structure was solved by direct methods. The phase set corresponding to the maximum figure of merit gave an E-map that could be interpreted in terms of the known cation stoichiometry of cumengéite. Insertion of the cation positions and refinement of the positional variables resulted in convergence at an *R* index of 34%. Most of the anions were located on the following difference Fourier map; refinement of these positions resulted in location of the remaining anions, and further refinement for an isotopic model converged at an *R* index of 15%. The isotropic temperature factor of Pb(5) was impossibly high, indicating far too much electron density at this site. The isotropic temperature factor for this site was fixed at the average value for all the Pb sites, and the occupancy of the position was refined, together

with all other variable parameters. Convergence occurred at an *R* index of 12% and the occupancy of the Pb(5) site was equal to 0.5.

It was at this stage that the long-exposure upper-level precession photographs were taken to make sure that there was not a weak supercell, and that the microprobe analysis was done to check for the presence of additional components. Isotropic refinements were continued in those tetragonal subgroups of *14/mmm* that led to a splitting of the Pb(5) into two symmetrically distinct sites; however, in all cases, both non-equivalent sets of sites were half-occupied.

The absorption correction was obviously not quite satisfactory, as indicated by the merging *R* indices. Consequently, a selection of small fragments was put through a sphere grinder, and an ellipsoidal crystal was used to collect a second set of intensity data. The cell dimensions of this crystal (not significantly different from the first) are given in Table II. The merging *R* index for the azimuthal

data was 3.7%, a great improvement over the first data set, and the merging *R* index for the normal data was 4.4%. In principle, the correction should be better than this, but the cumengéite tended to give very prolate ellipsoids on grinding, which combined with the very high absorption coefficient ($M = 359.6 \text{ cm}^{-1}$) to give considerable uncertainty to the absorption correction. Refinement in *I4/mmm* for an isothermal model gave an *R* index of 9.4%, again with a half-occupied Pb(5) site; non-centric tetragonal space groups also gave half-occupied sites, and we were forced to adopt the *I4/mmm* model. Temperature factors were converted to anisotropic, and full-matrix refinement of all variables resulted in convergence at an *R* index of 7.1% and a weighted *R* index of 5.5% for observed data. Final parameters are given in Tables III and IV, and observed and calculated structure factors are given in Table V.* Selected interatomic distances are given in Table VI.

Table VI. Selected bond lengths (Å) in cumengéite

Pb(1)-Cl(1)	2.81(1) x4	Pb(4)-Cl(2)a	3.084(7) x2
Pb(1)-Cl(3)	2.90(2) x2	Pb(4)-Cl(4)	3.024(2) x2
<Pb(1)-Cl>	2.84	Pb(4)-Cl(5)	3.26(1)
Pb(2)-Cl(4)	2.91(1) x4	Pb(4)-O(1)	2.45(2) x2
Pb(2)-Cl(5)	3.26(1) x4	Pb(4)-O(2)	2.51(2)
<Pb(2)-Cl>	3.09	<Pb(4)-Cl, O>	2.86
Pb(3)-Cl(2)	2.835(7) x2	Pb(5)-Cl(6)	2.94(1) x2
Pb(3)-Cl(2)a	3.132(7) x2	Pb(5)-Cl(2)a	3.402(7) x4
Pb(3)-Cl(5)	2.966(2) x2	Pb(5)-O(4)a	2.72(2) x2
Pb(3)-O(3)	2.60(3)	<Pb(5)-Cl, O>	3.12
<Pb(3)-Cl, O>	2.92		
Cu(1)-Cl(1)	2.993(5)	Cu(2)-Cl(1)	2.75(2)
Cu(1)-Cl(2)	2.855(7)	Cu(2)-O(1)	1.96(1) x4
Cu(1)-O(1)a	1.99(1)	<Cu(2)-O>	1.96
Cu(1)-O(2)	1.96(1)		
Cu(1)-O(3)	1.95(2)		
Cu(1)-O(4)	1.95(2)		
<Cu(1)-O>	1.96		
O(1).....Cl(1)	3.24(2)	O(3).....Cl(3)	3.22(2)
O(2).....Cl(5)	3.15(2)		

Discussion

Cation coordination. The cumengéite structure shows an amazingly diverse range of cation coordinations. Pb(1) has pseudo-octahedral coordination by six chlorine atoms. As Pb(1) lies on the 4-fold axis, the four equatorial bonds are equal, and all Cl-Pb(1)-Cl bond angles are 90°; the only departure from ideal octahedral geometry is a slight extension of the axial bonds relative to the equatorial bonds. Pb(2) also lies on the 4-fold axis, but is coordinated by eight chlorine atoms; these are arranged in a square antiprism, with the central cation displaced off-centre along the 4-fold axis.

* Table V is deposited in the Mineralogy Library, British Museum (Natural History), London SW7 5BD.

Pb(3) is coordinated by 6 chlorines and 1 oxygen atom, arranged in an augmented trigonal prism. Pb(3) lies on the mirror planes perpendicular to *X* and *Y*; four augmented trigonal prisms share corners to form a four-membered ring about the 4-fold axis. Pb(4) is co-ordinated by 5 chlorine and 3 oxygen atoms, arranged in a very distorted biaugmented trigonal prism. Pb(4) lies on the diagonal mirror planes, and Pb(4) polyhedra share corners to form a four-membered ring about the 4-fold axis. Pb(5), the half-occupied Pb site, lies on the mirror planes perpendicular to *X* and *Y*, and is coordinated by 6 chlorine and 2 oxygen atoms, arranged in a biaugmented trigonal prism. It is perhaps of significance that for Pb(3) and Pb(5), the basic trigonal prism consists of Cl atoms, and the augmented vertices are OH⁻ anions.

Cu(1) occupies a general position and is pseudo-octahedrally coordinated by 4 oxygen and 2 chlorine atoms. The 4 oxygens are actually OH⁻ anions and are in a square-planar arrangement around the central Cu(1) cation, with a mean Cu(1)-O distance of 1.96 Å. The 2 chlorine atoms are in a *trans* arrangement with a mean Cu-Cl distance of 2.92 Å. The resulting coordination is octahedral with a strong Jahn-Teller distortion. Cu(2) lies on a diagonal mirror plane and is coordinated by 4 oxygens and 1 chlorine atom; the

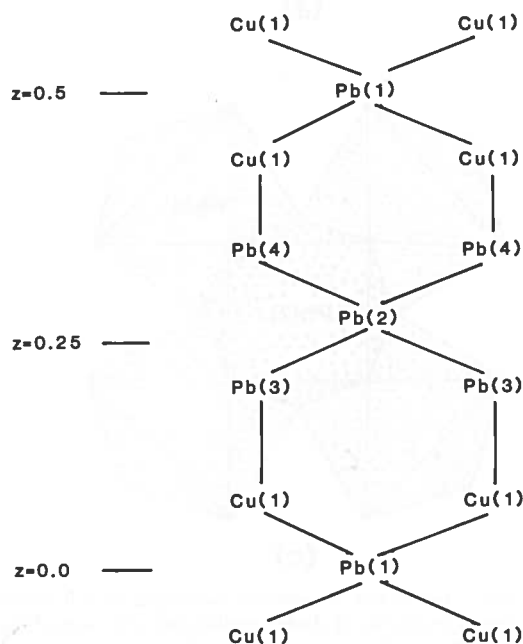


FIG. 1. The cation arrangement along one of the rods centred on a 4-fold axis.

oxygens are in a square-planar arrangement with a mean $\text{Cu}(2)\text{-O}$ distance of 1.96 Å, and the chlorine is 2.75 Å from $\text{Cu}(2)$ in an axial position, forming a slightly distorted square pyramid.

Structure description. Cumengéite is best described as a rod structure, with each rod centred on a 4-fold axis in the unit cell. The basic constitution of the rod is shown diagrammatically in fig. 1, and sections through the rod are shown in figs. 2(a-d). The $\text{Pb}(1)\text{Cl}_6$ octahedron lies on the 4-fold axis at the origin of the unit cell, and is

surrounded by a double-tiered necklace of edge-sharing $\text{Cu}(1)(\text{OH})_4\text{Cl}_2$ octahedra (fig. 2a); embedded in the outside of the necklace and promoting linkage between the upper and lower tiers is the $\text{Cu}(2)(\text{OH})_4\text{Cl}$ square pyramid, shown in fig. 2a by bond spokes rather than as polyhedra. This compact unit links upwards to another compact unit centred on the $\text{Pb}(2)\text{Cl}_8$ square antiprism. The lower section of this unit is the four-membered ring of corner-sharing $\text{Pb}(3)\text{Cl}_6(\text{OH})$ augmented trigonal prisms shown in fig. 2b. This links by

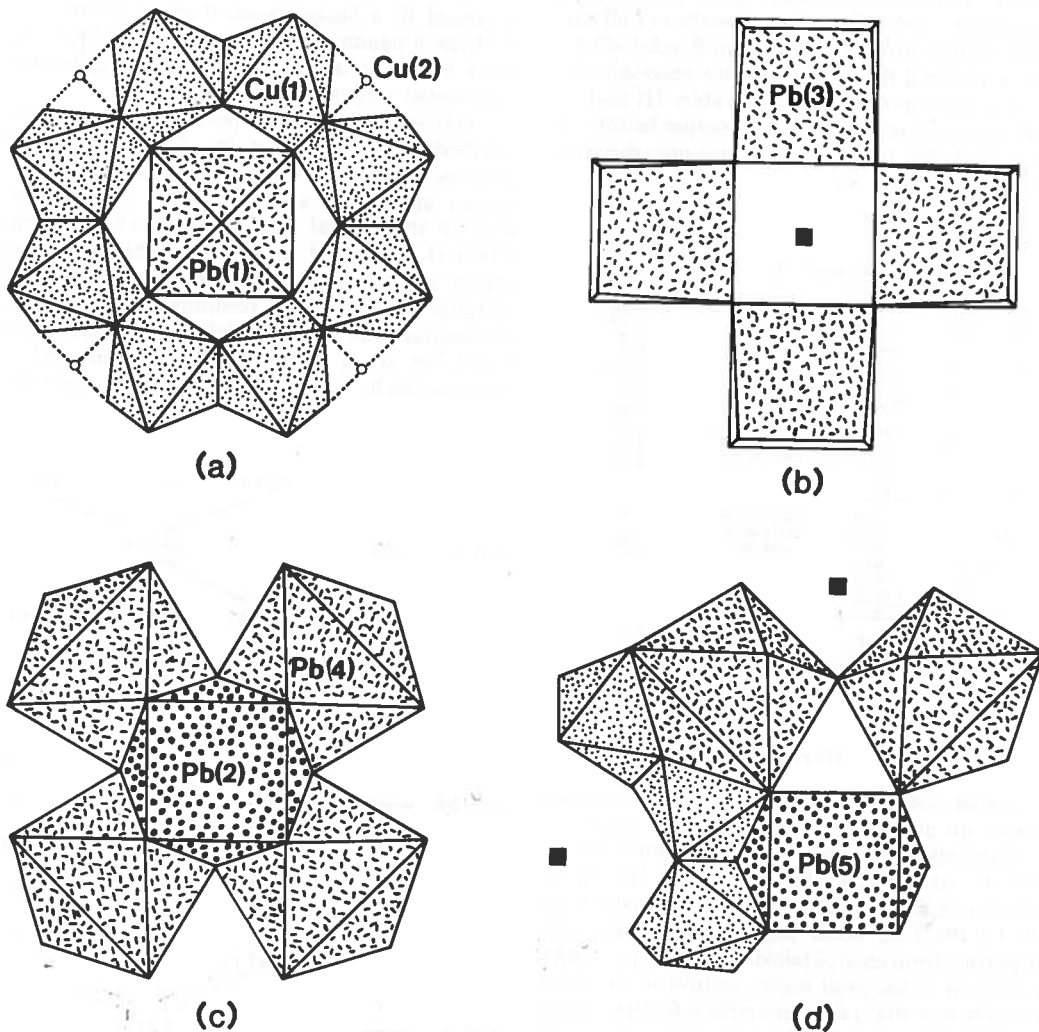


FIG. 2. (a) $\text{Pb}(1)\text{O}_6$ octahedron surrounded by a double-tiered necklace of edge-sharing $\text{Cu}(1)\text{O}_6$ octahedra; $\text{Cu}(2)\text{-O}$ bonds are shown by dashed spokes; (b) corner-linked ring of $\text{Pb}(3)\text{O}_7$ augmented trigonal prisms; the seventh anion underlies the prism in each polyhedron, and the 4-fold axis is shown; (c) $\text{Pb}(2)\text{O}_8$ square antiprism, girdled by four corner-linked $\text{Pb}(4)\text{O}_8$ dodecahedra; (d) $\text{Pb}(5)\text{O}_8$ polyhedron in the inter-rod position; adjacent rods are centred on the 4-fold axes shown.

Table VII. Empirical bond-valence* table for cumengéite

	Pb(1)	Pb(2)	Pb(3)	Pb(4)	Pb(5) [†]	Cu(1)	Cu(2)	H(1)	H(2)	H(3)	H(4)	Σ
Cl(1)	0.35 ^{x4}					0.12 ^{x4}	0.18					1.01
Cl(2)			0.41 ^{x2} 0.21 ^{x2}	0.19 ^{x2}	$\frac{0.22x4}{2}$	0.15						1.07
Cl(3)	0.31 ^{x2}									0.20 ^{x4}		1.11
Cl(4)		0.31 ^{x4}		0.20 ^{x2}								1.11
Cl(5)		0.21 ^{x4}	0.26 ^{x2}	0.16					0.20			1.09
Cl(6)					$\frac{0.37x2}{2}$			0.20 ^{x4}				1.17
O(1)				0.37 ^{x2}		0.41	0.45 ^{x4}	0.80				2.03
O(2)				0.32		0.45 ^{x2}			0.80			2.02
O(3)			0.27			0.47 ^{x2}				0.80		2.01
O(4)					$\frac{0.26x2}{2}$	0.47 ^{x2}					1.00	2.07
Σ	2.02	2.08	2.03	2.00	1.05	2.07	1.98	1.00	1.00	1.00	1.00	

* bond-valences in v.u., calculated from the curves of Brown (1981), with the exception of Pb-Cl bonds (see text), and H-bonds which were assigned as 0.80 and 0.20 v.u. to donor and acceptor bonds respectively.

[†] half-occupied site.

edge-sharing to the base of the Pb(2)Cl₈ square antiprism, which links by edge-sharing to a four-membered corner-sharing ring of Pb(4)(OH)₃Cl₅ polyhedra (fig. 2c). This unit then links to the base of a [Cu(1)(OH)₃Cl] necklace, and the sequence in the upper half of the unit cell is the mirror equivalent of that in the lower half (fig. 1).

These rods form a body-centred array, and share polyhedral edges and corners to form a continuous three-dimensional structure. Further linkage is provided by the half-occupied Pb(5) site (fig. 2d) in an inter-rod position. The structure is strongly related to that of boléite (Rouse, 1973), but a detailed examination of structural relations in the (Pb,Cu) oxy-chloride minerals will be deferred to a later paper.

Hydrogen bonding. An empirical bond-valence analysis is given in Table VII. This analysis uses the curves of Brown (1981) for Pb-O, Cu-O, and Cu-Cl bonds; there are no published curves for Pb-Cl bonds. When no bond-valence curves are available, Brown and Shannon (1973) suggest using a relationship of the form

$$\text{b.v.} = S_0 \left(\frac{R_0}{R} \right)^{-N} \quad (1)$$

where S_0 is the formal Pauling bond strength
 R_0 is the observed mean bond length
 R is the individual bond length
 N is an 'appropriate' exponent.

To derive an appropriate value for N , note that

Pb(1)-Cl(3) \sim Pb(2)-Cl(4) and thus the bond-valences for these two bonds will be approximately equal. Equating the bond-valence equations from (1) and solving for N gives $N \sim 3.5$; this value was used in Table VII, and seems to be fairly satisfactory.

Although the H positions were not determined in this study, a sensible hydrogen-bonding scheme can be derived from the local geometry and anion bond-valence requirements (Table VII). Hydrogen bonding is particularly important with regard to satisfying the bond-valence requirements around the Cl(3) and Cl(6) anions, bond-valence sums of ~ 0.35 v.u. occurring at both these anions if hydrogen bonding is not taken into account.

Acknowledgements. Financial support for this study was provided by the Natural Sciences and Engineering Research Council of Canada, in the form of a fellowship, an operating grant and a major equipment grant to F.C.H., and by the University of Manitoba, in the form of a graduate fellowship to L.A.G.

REFERENCES

- Abdul-Samad, F. A., Humphreys, D. A., Thomas, J. H., and Williams, P. A. (1981) *Mineral. Mag.* **44**, 101-4.
- Brown, I. D. (1981) In *Structure and Bonding in Crystals, II* (M. O'Keefe and A. Navrotsky, eds.). Academic Press, New York, 1-30.
- and Shannon, R. D. (1973) *Acta Crystallogr.* **A29**, 266-82.

- Cromer, D. T., and Liberman, D. (1970) *J. Chem. Phys.* **53**, 1891-8.
- and Mann, J. B. (1968) *Acta Crystallogr.* **A24**, 321-4.
- Dean, A. C., Symes, R. F., Thomas, J. H., and Williams, P. A. (1983) *Mineral. Mag.* **47**, 235-6.
- Hawthorne, F. C. (1985) *Ibid.* **49**, 85-91.
- Humphreys, D. A., Thomas, J. H., Williams, P. A., and Symes, R. F. (1980) *Ibid.* **43**, 901-4.
- Rouse, R. C. (1973) *J. Solid State Chem.* **6**, 86-92.
- Winchell, R. E., and Rouse, R. C. (1974) *Mineral. Rec.* **5**, 280-7.

[Manuscript received 25 April 1985;
revised 19 June 1985]